

Electronic structure and optical properties of amorphous Se and Te

A. Vaidyanathan*

Department of Physics, University of Rhode Island, Kingston, Rhode Island 02881

S. S. Mitra and Y. F. Tsay†

Department of Electrical Engineering, University of Rhode Island, Kingston, Rhode Island 02881

(Received 28 September 1978)

The electronic energy-band structures and densities of states of trigonal Se and Te are calculated using the empirical pseudopotential method. The amorphous phases of these materials are simulated by a model in which the interchain distances are allowed to have a Gaussian distribution centered at 108% of the trigonal distance for Se and 104% of the corresponding distance for Te, while the intrachain distances are kept fixed at the trigonal values. The amorphous densities of states are obtained by calculating the crystalline densities of states for five different values of the second-nearest-neighbor distances and averaging these densities of states by using Gaussian weighting functions. The nondirect transition model and energy-dependent matrix elements are used to calculate the imaginary parts of the dielectric functions of amorphous Se and Te. The results are compared with the results of other calculations and experiments.

I. INTRODUCTION

For more than a decade there has been considerable interest in the electronic properties of crystalline and amorphous (a-) Se and Te. Even though the two materials have been well studied experimentally, there have been only a few theoretical calculations of the electronic properties of the amorphous phases of these two materials. As explained in Sec. II, results of these calculations are at variance with each other and with the experimental results, regarding bandwidths and structures in the electronic densities of states.

In an attempt to improve this situation, we have calculated the electronic densities of states of amorphous Se and Te using a model incorporating local-density disorder that introduces Gaussian distributions in the interchain distances, while the intrachain distances are kept fixed. The resulting imaginary parts of the dielectric functions are calculated using the nondirect transition model and energy-dependent oscillator strengths. The results are compared with the results of other calculations and experiments.

II. SURVEY OF CURRENTLY AVAILABLE RESULTS ON BAND STRUCTURES AND DENSITIES OF STATES OF a-Se AND a-Te

Kramer *et al.*^{1(a)} were the first to calculate the electronic densities of states of amorphous Se and Te. They assumed that the amorphous forms retained the trigonal nearest-neighbor arrangements and simulated the loss of long-range order by

Gaussian broadening of the reciprocal lattice vectors in \vec{k} space. Employing the pseudopotential method and Green's-function techniques they obtained, for the amorphous materials, bands that were broadened near the band gaps and which remained sharp away from the gaps. It was not clear whether this broadening was an artifact of the model or whether intrinsic physical significance should be attributed to it. Furthermore, the energies of the valence bands were quite doubtful.^{1(a)} The resulting densities of states retained some fine structures in the regions of the top two valence bands and the first conduction bands, which had p -like symmetry, while the second-conduction-band triplets were essentially structureless. This result was in good agreement with the results of photoemission experiments carried out by Laude *et al.*^{1(b)}

Hartmann and Mahanti² calculated the density of states of amorphous Te by a tight-binding approximation. They assumed the trigonal unit cell was retained in the amorphous form, and introduced disorder by distorting the unit cell at its ends. The p_2 band in this calculation exhibited three sharp peaks absent in the Kramer *et al.*^{1(a)} calculations. Furthermore, their p_1 and p_3 bands consisted of only one broad peak with a small shoulder on the high-energy side, while the results of Kramer *et al.* had two peaks in each of these bands.

Nielsen³ probed the valence bands of amorphous Se by vacuum photoemission using 21.2 eV photons. His experiment indicated that the entire valence-band width of amorphous Se was no more than 9 eV, in contradiction with Kramer's result, which

indicated that the upper two valence bands alone had a width of 8 eV. Chen⁴ calculated the energy-band structure of Se chains and rings using hybrid orbitals and semiempirical Hamiltonian matrix elements. The effects of disorder were treated by imposing a Gaussian distribution on each energy level, assuming short-range order. The resulting density of states was in excellent agreement with that of Nielsen's photoemission experiment. This calculation predicted complete merging of the *s*- and *p*-like valence bands, in disagreement with the Kramer *et al.*^{1(a)} result according to which these bands were well separated.

Shevchik *et al.*⁵ measured the entire valence-band densities of states of trigonal and amorphous Se and Te employing 1486.6 eV x ray, and 40.8 and 21.2 eV ultraviolet photoemission. They found that the density of states of trigonal Se, and not amorphous Se, was in good agreement with Kramer's result for amorphous Se. Also contrary to the Kramer *et al.* results, there was no broadening in the amorphous density of states relative to the crystalline density of states. Furthermore, the results of Shevchik *et al.* did not show the merging of *s*- and *p*-like bands proposed by Chen. Shevchik *et al.* favored the idea that amorphous Se was composed of chains and Se rings in a relative proportion which depended on the preparation conditions.

Schluter *et al.*⁶ performed photoemission experiments on trigonal and amorphous Te and found that the dip in the crystalline density of states filled up in the amorphous state. This result differed from the photoemission data of Shevchik *et al.* who found that the above-mentioned dip became more pronounced in the amorphous phase both in Se and Te. They also predicted that the presence of sixfold rings led to the dip deepening, while eightfold rings caused the dip to fill up. They concluded that the amorphous Se samples used by Shevchik *et al.* contained a majority of sixfold rings. Ichikawa⁷ measured the x-ray photoemission spectra of trigonal and amorphous Te and found the general features of the two densities of states very similar. Joannopoulos *et al.*⁸ calculated the densities of states of trigonal Se and Te using the empirical pseudopotential method (EPM) and tight-binding models and analyzed the changes observed in the photoemission spectra of the same materials due to disorder. They disagreed with the Shevchik *et al.* suggestion of the presence of substantial numbers of eightfold rings, and favored the idea of the presence of five-, six-, and sevenfold rings.

Thus one can see that there is no general agreement between the currently available results regarding the structural models and densities of

states of amorphous Se and Te. In Sec. III we present a local-density-disorder model for a-Se and a-Te that reproduces the experimental densities of states and dielectric response functions of these two materials reasonably well. The local-density-disorder model has been used in the past by Tsay *et al.*⁹ to predict successfully the densities of states and optical properties of amorphous III-V semiconductors.

III. STRUCTURES OF AMORPHOUS Se AND Te

Before discussing the structural model for amorphous Se and Te used in this work, let us look at the structures of the trigonal phases and the experimental data relating to the structures of the amorphous states of these materials.

The crystal structures of trigonal Se and Te consist of helical chains that spiral around the crystalline *c* axis.¹⁰ The helices are arranged in an hexagonal array, the space group being D_3^4 or D_3^6 , depending on the sense of rotation. Each atom is tightly covalently bonded to two atoms on the same chain and rather weakly bonded to four atoms on the neighboring chains. Richter¹¹ found, from x-ray diffraction measurements, that a-Se had the same structural element as the trigonal crystal. He also noticed that samples of a-Se prepared by different methods had different interchain distances, while the intrachain distances remained the same as the trigonal value. The shortest distance between atoms belonging to adjacent chains was found to be 3.45 Å in the crystal and 3.69 and 3.86 Å, respectively, in amorphous samples prepared by two different methods. Kaplow *et al.*¹² obtained radial distribution functions (RDF) of amorphous and trigonal Se from x-ray diffraction measurements. The intrachain and interchain bond distances in the crystal were 2.32 and 3.47 Å. The corresponding values obtained for the amorphous material were 2.34 and 3.75 Å, respectively.

From an experimental study of the imaginary part of the dielectric function of a-Te, Stuke¹³ suggested that the structure is composed of randomly arranged chains in which the interchain bonding is weaker than in trigonal Te, but the intrachain bonding is stronger. From Raman spectra of a-Te, Lucovsky¹⁴ concluded that the binding in a-Te is more molecular than in trigonal Te. This could be caused by an increase in interchain bond distance and/or a decrease in intrachain bond distances. Ichikawa¹⁵ conducted electron-diffraction studies of a-Te films and found that the intrachain bond distance decreased to 2.8 Å from the trigonal value of 2.835 Å, while the interchain distance increased to 3.65 Å from the trigonal value of 3.5 Å.

Thus the experimental evidence is convincing that in both Se and Te, in going from the trigonal form to the amorphous form, the intrachain distances are essentially unaltered, while the chains themselves are pulled apart from each other. It is also to be noted that the changes in the interchain distances are approximately 8% and 4% of the trigonal values for Se and Te, respectively. The experimental^{12,15} radial-distribution function for a-Se and a-Te also indicate that the first- and second-nearest-neighbor distances (which correspond to the shortest intra- and interchain distances, respectively) obey Gaussian distribution functions. In view of these experimental findings, we chose a model for a-Se and a-Te where the intrachain and interchain distances were allowed to have Gaussian distributions centered at the trigonal intrachain distances, and 108% of the trigonal

interchain distance for Se and 104% of the trigonal interchain distance for Te, respectively.

IV. ELECTRONIC BAND STRUCTURES AND OPTICAL PROPERTIES OF AMORPHOUS Se AND Te

Using the pseudopotential form factors of Kramer *et al.*^{1(a)} as a starting point, we first calculated the band structures and densities of states of the trigonal crystals. The form factors were adjusted until a good agreement between the structures in the calculated and experimentally^{5,6} deduced densities of states was obtained. The density of states obtained using 900 \vec{k} points in the irreducible part of the Brillouin zone with no broadening function is shown in Fig. 1. Our final results for the band structures of the trigonal crystals, which are in agreement with those of

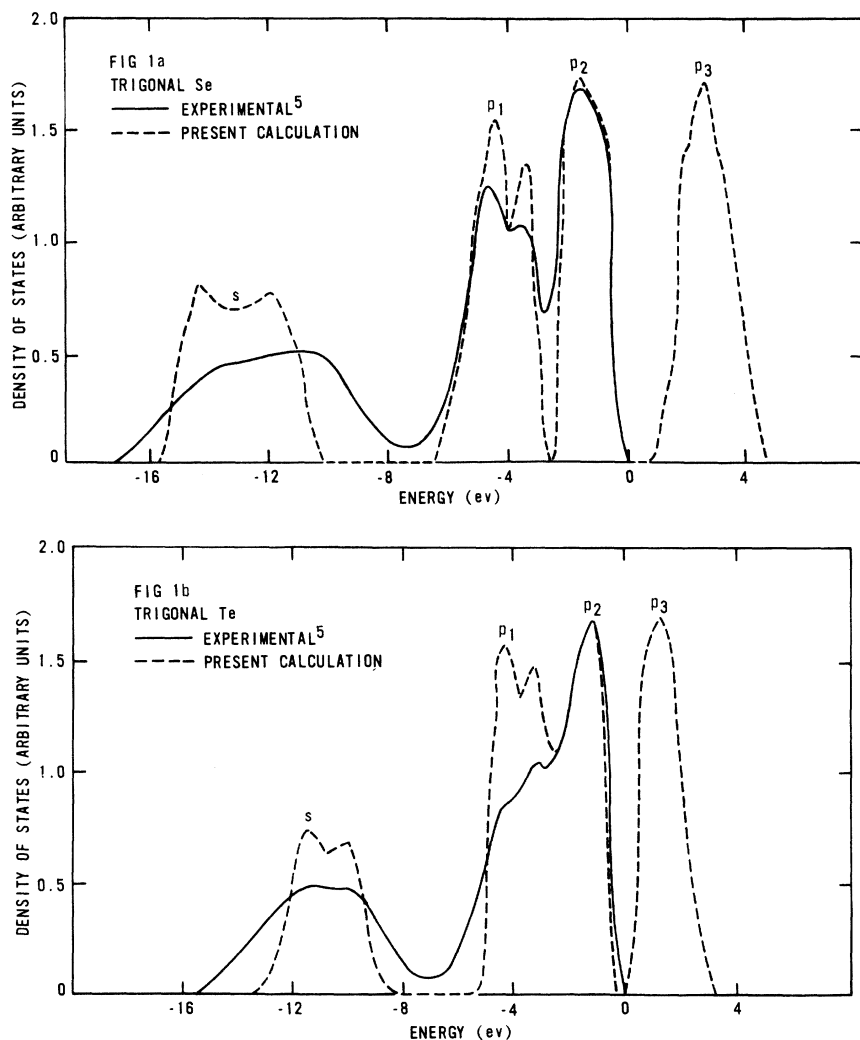


FIG. 1. (a) Electronic density of states of trigonal Se. (b) Electronic density of states of trigonal Te.

Joannopoulos *et al.*,⁸ are shown in Fig. 2. Using these form factors, properly scaled, calculations were repeated for five different values of the first- and second-nearest-neighbor distances. The band structures of the trigonal Se and Te crystals when the interchain distances are increased by 8% and 4%, respectively, keeping the intrachain distances fixed are shown by the dashed curve in Fig. 2. One can see that there are noticeable changes from the band structures of the normal trigonal crystals. The resulting densities of states were averaged using weighting functions of the form⁹

$$\exp\left[-0.5\left(\frac{r_1-r_{1a}}{\sigma_1}\right)^2 + \left(\frac{r_2-r_{2a}}{\sigma_2}\right)^2\right],$$

where r_{1a} and r_{2a} are, respectively, the first- and second-nearest-neighbor distances (which correspond to the shortest intrachain and interchain distances) in the amorphous materials, and σ_1 and σ_2 are the spread of the first and second peaks in the amorphous RDF due to disorder. r_{1a} was set equal to the trigonal r_1 for both Se and Te, while r_{2a} was taken to be 108% of the trigonal r_2 for Se and 104% of the trigonal r_2 for Te, for reasons explained earlier. σ_1 and σ_2 were determined from the ex-

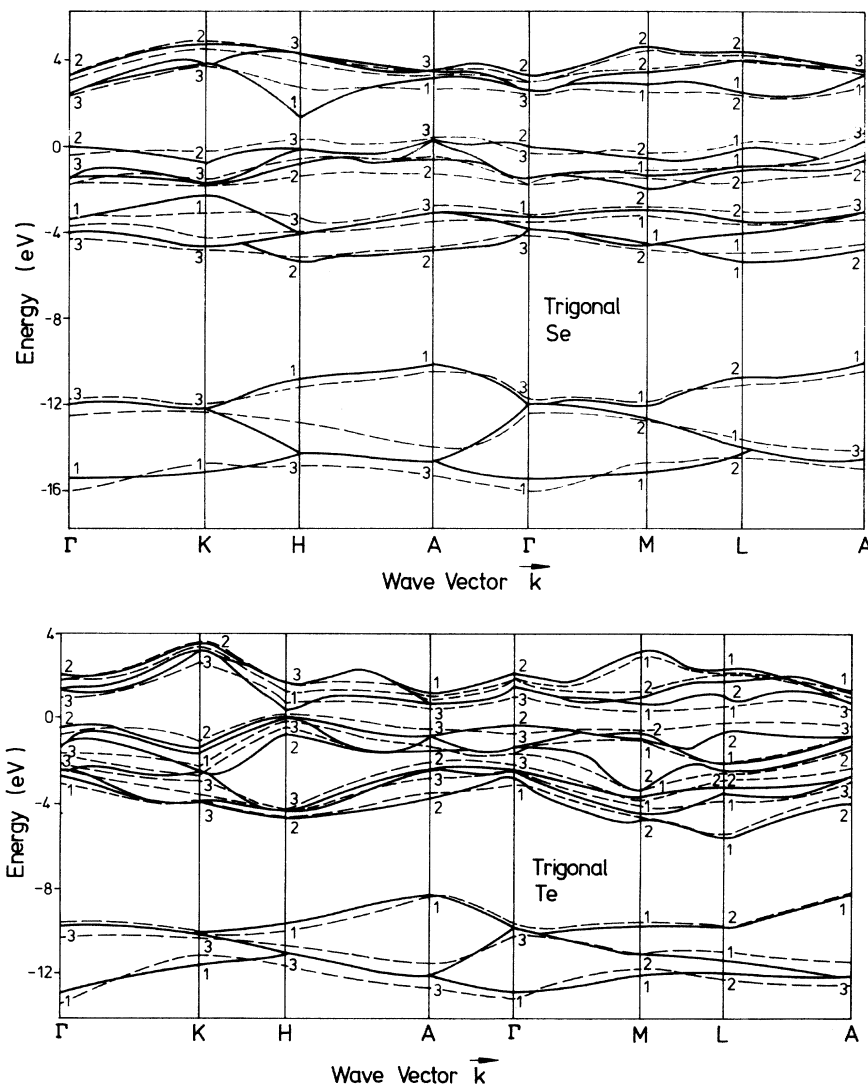


FIG. 2. (a) Band structure of trigonal Se (full lines). Dashed lines represent band structure of a crystal with 8% increase in interchain distance. (b) Band structure of trigonal Te (full lines). Dashed lines represent band structure of a crystal with 4% increase in interchain distance.

perimental RDF's with the help of the relation⁹

$$\sigma_i^2 = \sigma_{i\text{am}}^2 - \sigma_{i\text{thermal}}^2 \approx \sigma_{i\text{am}}^2 - \sigma_{i\text{crystal}}^2, \quad i = 1, 2.$$

From the experimentally^{12,15} determined RDF's the values shown in Table I were obtained for the various σ 's. Calculated densities of states for the two disordered elements are compared with those deduced from the photoemission experiments^{5,6} in Fig. 3.

Our results favor the density of states obtained by Kramer *et al.*¹ using the empirical pseudopotential method, over those of Hartmann and Mahanti,² who used a tight-binding approximation, and of Chen,⁴ who employed molecular orbitals. For a-Se the width of the *p*-like valence bands in our calculation is about 7 eV, which is close to Kramer's value of 8 eV. Chen's theoretical results, which agreed with Nielsen's³ observation that the

TABLE I. Relevant structural parameters for amorphous Se and Te. All σ 's are in \AA units.

	σ_{1a}	σ_{1c}	σ_1	σ_{2a}	σ_{2c}	σ_2
Se(Ref. 12)	0.125	0.08	0.096	0.2	0.16	0.12
Te(Ref. 15)	0.125	0.1	0.07	0.138	0.1	0.095

entire valence-band width of a-Se was no more than 9 eV, is at variance with our result as well as the recent photoemission experiments,⁵ in which the *p*-like valence bands had a width of 8 eV and the *s*-like bands, 10 eV. Nielsen's experiment obviously did not detect the *s* bands and this is due to the fact⁵ that Nielsen used 21.2 eV photons and the electrons emitted from the lower *s* bands had energy 8 eV above the top of the valence

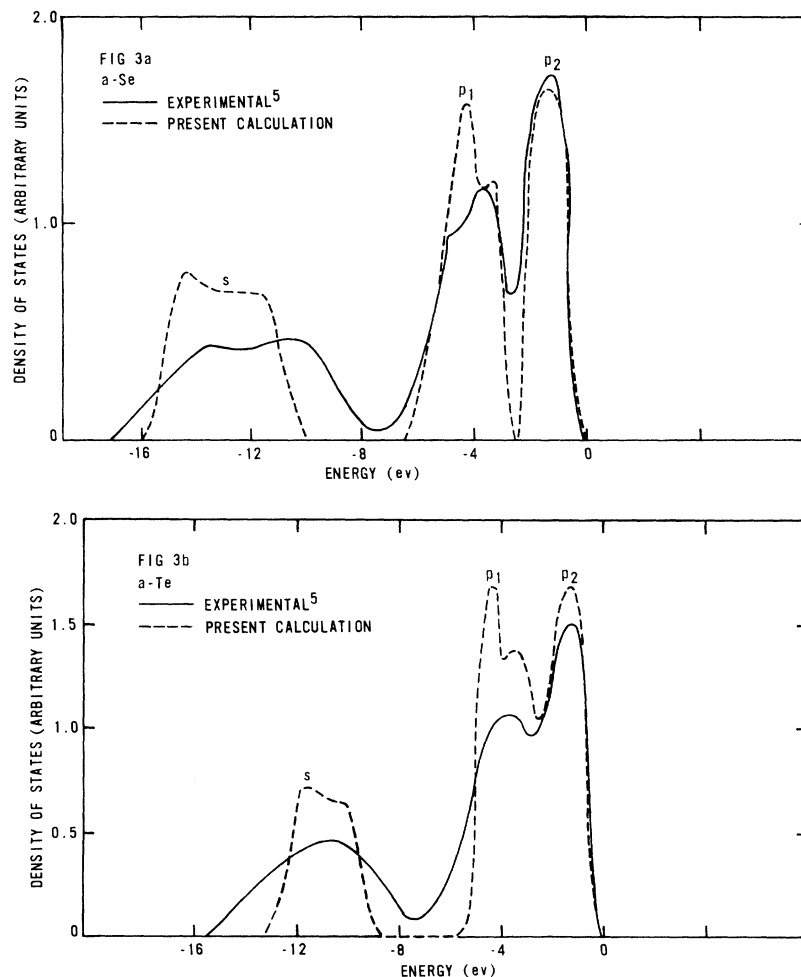


FIG. 3. (a) Electronic density of states of amorphous Se. Solid line curve is the experimental result (Ref. 5). Dashed curve is the result of the present calculation. (b) Electronic density of states of amorphous Te. Solid line curve is the experimental result (Ref. 6). Dashed curve is the result of the present calculation.

band, which overlapped with a minimum in the conduction band density of states. The merging of s - and p -like bands proposed by Chen is not supported by our calculation. The recent photoemission experiments⁵ did not show this merging either. For a -Te, the triplet structure in the p_2 bands predicted by Hartmann and Mahanti² is not obtained in our calculation or in the recent experiments,^{5,6} in accordance with Kramer's result. This structure probably resulted from Hartmann and Mahanti's assumption of perfect short-range order which vanished abruptly beyond a given cluster. A gradual loss of crystalline order with increasing distance would be more realistic. The p_1 peak in our calculation is a doublet, in accordance with Kramer's result, but is shifted towards

lower energy by about 1 eV. However, our p_3 peak is a singlet, in closer agreement with Hartmann and Mahanti's result than with that of Kramer *et al.*

On comparing the crystalline and amorphous densities of states obtained in this calculation, we note the following: The doublet structure in the p_1 -like states is preserved. However, the lower-energy peak is enhanced in strength while the higher-energy peak is diminished. This is due to the fact that these two peaks are associated with intrachain and interchain bonding states, respectively. When the chains are pulled apart, the interchain bonding becomes weaker and more electrons are localized within the chains.

Photoemission experiments^{5,6} reveal this be-

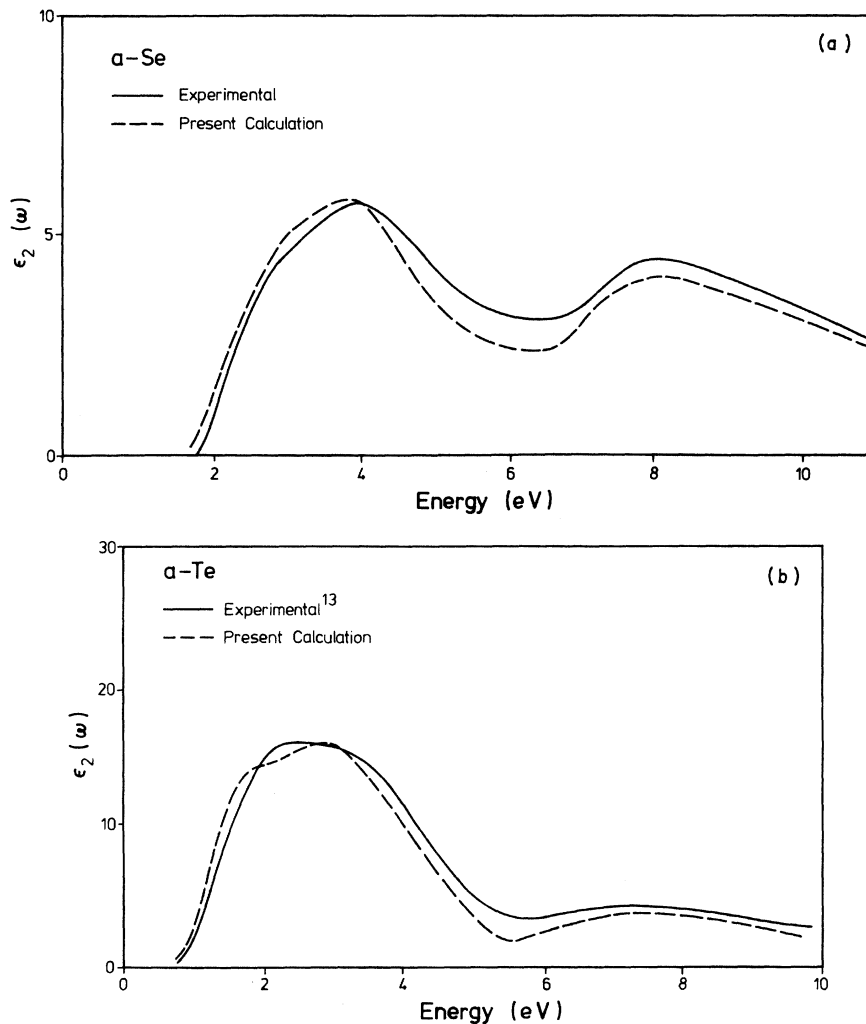


FIG. 4 (a) Imaginary part of the complex dielectric response function [$\epsilon_2(\omega)$] of amorphous Se. Solid line curve is the experimental result (Ref. 18). Dashed curve is the result of the present calculation. (b) Imaginary part of the complex dielectric response function [$\epsilon_2(\omega)$] of amorphous Te. Solid line curve is the experimental result (Ref. 13). Dashed curve is the result of the present calculation.

havior in a-Te, but the opposite in a-Se. The effect of pulling the chains apart is to weaken the Van der Waals bonding between the chains and strengthen the covalent bonds in the chains. Experiments¹⁴ show that the bonding in a-Te is indeed more covalent than in trigonal Te. The agreement between our results and the experimental findings on a-Te suggest that our model for a-Te is quite adequate. In the case of Se, it has long been believed^{3,12,14} that a-Se consisted of chains and rings in relative proportions, which depended on the method of sample preparation. Our model contains only the chains found in the trigonal form and does not include the rings found in the monoclinic form. In order to explain all of the experimental findings on a-Se, a model incorporating both chains and rings is needed. Unfortunately, the unit cell of monoclinic Se contains a large number of atoms, and this makes empirical pseudopotential calculations of it extremely complicated.^{1(b)} We also note that, in going from the trigonal to the amorphous form, the states on the high-energy side of the *s*-like peak associated with interchain states are lowered in energy towards the intrachain states, causing the dip to fill up. While the experiments of Schluter *et al.*⁶ show that the dip does fill up, those of Shevchik *et al.*⁵ show that the dip deepens. This discrepancy has been explained⁸ as being due to the presence of sixfold rings deepening the dip, while eightfold rings fill up the dip. Our model does not assume the presence of odd- or even-membered rings, and hence is incapable of making any explicit con-

clusion about the nature of the rings. The filling up of the dip in our calculation is due to the weakening of interchain bonds, causing a transfer of electrons from between the chains to inside the chains.

The imaginary parts of the dielectric functions [$\epsilon_2(\omega)$] for the two amorphous materials were calculated using the nondirect transition model¹⁶ and energy-dependent oscillator strengths.¹⁷ The results are compared with those deduced from the reflectivity measurements of Leiga¹⁸ and Stuke¹³ in Fig. 4. The agreement is seen to be good.

V. CONCLUSION

The empirical pseudopotential method is combined with a local-density-disorder model to predict the electronic density of states and dielectric response functions of amorphous Se and Te. The experimental results favor pseudopotential calculations over tight-binding and molecular-orbitals methods. The results of the pseudopotential calculation are significantly improved when the pseudopotential form factors are obtained by fitting the theoretical density of states to the experimental result, and the model used for the amorphous materials is closely related to available structural information.

ACKNOWLEDGMENT

This research was supported in part by AFCRL Contract No. F19628-75-C-0163.

*Present address: Air Force Weapons Laboratory, Kirtland AFB, New Mexico 87117.

†Present address: Institute for Aerospace Studies, University of Toronto, 4925 Dufferin Street, Downsview, Ont., Canada M3H5TG.

^{1a}B. Kramer, K. Maschke, and L. D. Laude, *Phys. Rev. B* **8**, 5781 (1973), and references therein.

^{1b}L. D. Laude, B. Kramer, and K. Maschke, *Phys. Rev. B* **8**, 5794 (1973).

²W. M. Hartmann and S. D. Mahanti, *J. Non-Cryst. Solids* **8-10**, 633 (1972).

³P. Nielsen, *Phys. Rev. B* **6**, 3739 (1972).

⁴I. Chen, *Phys. Rev. B* **7**, 3672 (1973).

⁵N. J. Shevchik, M. Cardona, and J. Tejeda, *Phys. Rev. B* **8**, 2833 (1973), and references therein.

⁶M. Schluter, J. D. Joannopoulos, M. L. Cohen, L. Ley, S. Kowalczyk, R. Pollak, and D. A. Shirley, *Solid State Commun.* **15**, 1007 (1974), and references therein.

⁷I. Ichikawa, *J. Phys. Soc. Jpn.* **36**, 1213 (1974).

⁸J. D. Joannopoulos, M. Schluter, and M. L. Cohen, *Phys. Rev. B* **11**, 2186 (1975), and references therein.

⁹Y. F. Tsay, D. K. Paul, and S. S. Mitra, *Phys. Rev. B* **15**, 4007 (1977).

¹⁰J. C. Slater, *Quantum Theory of Molecules and Solids* (McGraw-Hill, New York, 1965), Vol. 2, p. 49.

¹¹H. Richter, *J. Non-Cryst. Solids* **8-10**, 388 (1972).

¹²R. Kaplow, T. A. Rowe, and B. L. Averbach, *Phys. Rev.* **168**, 1068 (1968).

¹³J. Stuke, *J. Non-Cryst. Solids* **4**, 1 (1970).

¹⁴G. Lucovsky, A. Mooradian, W. Taylor, G. B. Wright, and R. C. Keezer, *Solid State Commun.* **5**, 113 (1967).

¹⁵T. Ichikawa, *Phys. Status Solidi B* **56**, 707 (1973).

¹⁶J. Tauc, *Optical Properties of Solids*, edited by S. Nudelman and S. S. Mitra (Plenum, New York, 1969).

¹⁷K. Maschke, and P. Thomas, *Phys. Status Solidi* **41**, 743 (1970); B. Kramer, K. Maschke, P. Thomas, and J. Treusch, *Phys. Rev. Lett.* **25**, 1020 (1970).

¹⁸A. G. Leiga, *J. Opt. Soc. Am.* **58**, 1441 (1968).